Journal of Metals, Materials and Minerals, 37(1), e2792, 2027

Surface hardness improvement of SUS430 stainless steel by solution nitriding and nitrocarburizing

Tanabodee PRADITJA[1,2], Patama VISUTTIPITUKU[1], Jatupon OPAPAIBOON[1], Prasonk SRICHAROENCHAI[1], Nipon TAWEEJUN[2] and Nithi SEENENARJHAN[1,*]

[1] *Department of Metallurgical Engineering, Faculty of Engineering, Chulalongkorn University, Bangkok, 10330, Thailand*
[2] *Thai Tohken Thermo Co., Ltd, Chonburi, 20000, Thailand*

***Corresponding author e-mail**: Nithi.S@chula.ac.th

Received date:
23 June 2026
Revised date:
22 July 2026
Accepted date:
29 September 2026

Keywords:
Heat Treatment;
Ferritic stainless steel;
Gas nitrocarburizing;
Solution nitriding;
SUS430 stainless steel

Abstract

This research aims to study the effect of the gas nitrocarburizing process on surface hardness and microstructural changes of ferritic stainless steel SUS430 (0.09% C and 16.44% Cr). The specimens were initially prepared by a solution nitriding process at 1050°C for 90 min, followed by cooling with nitrogen gas. After that, they were subjected to a gas nitrocarburizing process at 570°C for 180 min. The results show that this process can significantly improve the surface hardness, to a maximum hardness of 1341 HV, which is an increase of 774 HV compared to the specimen treated only by solution nitriding. The treatment at 1050°C led to the formation of a martensitic structure near the surface, which has high hardness and enhances the diffusion ability of nitrogen and carbon during the subsequent process. This diffusion resulted in the formation of a compound layer, including $Fe_{2-3}N$, Fe_4N, and CrN, along with a uniform diffusion zone. These are the key mechanisms responsible for the significant increase in surface hardness. The study indicates that the combination of solution nitriding and gas nitrocarburizing is an effective approach to improve the surface hardness of SUS430 stainless steel and shows high potential for industrial applications requiring wear and friction resistance.

1. Introduction

Stainless steel is an important engineering material widely used in industry due to its excellent corrosion resistance [1,2], along with mechanical properties suitable for various applications [3]. In particular, the ferritic stainless steel grade SUS430, which contains chromium as the main alloying element [2], can form a protective oxide film on the surface. This provides good corrosion resistance and allows its use in moderately high-temperature environments [4]. However, surface hardness remains a key limitation, especially in applications involving high wear and friction [5–7].

In industry, various heat treatment processes have been developed to improve surface properties. The solution nitriding process can increase surface hardness to approximately 550 HV to 650 HV [8,9], but it still has limitations in providing long-term wear resistance. Meanwhile, surface hardening processes such as nitriding and nitrocarburizing have gained increasing attention, as they can enhance surface properties without significantly affecting the bulk structure. In particular, gas nitrocarburizing [10] involves the diffusion of nitrogen and carbon into the steel surface at temperatures below the eutectoid temperature, resulting in the formation of both a compound layer and an underlying support diffusion zone [11–14]. This significantly improves surface hardness [2] and wear resistance [15,16].

However, previous studies on the application of gas nitrocarburizing to SUS430 stainless steel, based on Japanese industrial standards, have reported some limitations in practical use, particularly in terms of surface layer uniformity [6] and achievable hardness. Although gas nitrocarburizing has been widely investigated, relatively few studies have examined the use of solution nitriding as a pre-treatment prior to gas nitrocarburizing, particularly for SUS430 stainless steel. The martensitic structure formed during solution nitriding may provide favorable conditions for the subsequent diffusion of nitrogen and carbon during gas nitrocarburizing, potentially promoting the formation of a multilayered hardened surface structure. Therefore, this research focuses on combining solution nitriding with gas nitrocarburizing to evaluate their effects on microstructure and surface hardness, as well as to analyze their potential for industrial applications. A direct comparison with gas nitrocarburizing alone is also included to clarify the additional benefit of solution nitriding as a pre-treatment. The combined treatment is expected to improve surface hardness and wear performance compared with gas nitrocarburizing alone, thereby providing a potential two-step surface treatment approach for enhancing the performance and service life of SUS430 components [15].

2. Materials and methods

The material used in this study was ferritic stainless steel grade SUS430, which contains more than 16 wt% chromium [2]. The chemical composition is shown in Table 1.

The cold-rolled steel bar was cut into cylindrical specimens with a diameter of 22 mm and a thickness of 10 mm. The surfaces were then prepared up to 2000-grit sandpaper to remove oxide layers and

cutting marks before being subjected to heat treatment processes, namely solution nitriding and gas nitrocarburizing.

The initial microstructural examination of the as-received specimen, which was etched with a nitric-hydrochloric acid solution (10 mg nitric acid mixed with 30 mg hydrochloric acid) for approximately 3 s, revealed that the matrix consisted of ferrite, with spheroidal carbides dispersed throughout the microstructure [4], as shown in Figure 1. The average initial hardness was 251 HV, which was used as a baseline for comparison with the results after heat treatment.

2.1 Heat treatment process

In the first stage of heat treatment, the specimens were hardened in a vacuum furnace using the solution nitriding (SN) process. The treatment began with heating to 950°C and holding for 30 min to homogenize the initial microstructure, reduce residual stresses from previous processes, and prepare the material structure. The temperature was then increased to 1050°C [8,17] and held for 90 min under a pressure of 80 kPa, while nitrogen gas was introduced for 60 min to allow nitrogen diffusion into the specimen surface [18]. At this temperature, an austenitic structure is formed along with the dissolution of carbides, resulting in a solid solution state with dissolved nitrogen. Afterward, the temperature was reduced to 950°C and held for 30 min to stabilize the nitrogen-enriched austenite structure, promote a more uniform distribution of nitrogen within the surface layer, and reduce residual stresses in the specimen. Finally, the specimens were rapidly cooled to room temperature using nitrogen gas, as shown in Figure 2.

Subsequently, the specimens underwent a second heat treatment using the gas nitrocarburizing (NC) process, as illustrated in Figure 3, at 570°C [12,19–21] for 180 min. The flow rates of ammonia gas and endothermic gas were controlled equally at 10 $m^3 \cdot h^{-1}$. This continuous heat treatment process is designated as SN+NC.

2.2 Testing and characterization

Microstructural observation was carried out by sectioning the cylindrical specimens, after solution nitriding and nitrocarburizing, along the cross-section. The samples were then mounted in resin and polished to a final finish using 1 µm alumina powder. After that, the surfaces were etched with a nitric-hydrochloric acid solution (10 mg nitric acid mixed with 30 mg hydrochloric acid) for approximately 3 s to reveal the microstructure. The observations were performed using an optical microscope (Nikon MM-400) at both the surface and core regions.

Detailed microstructural analysis and elemental distribution were examined using a scanning electron microscope (SEM) [22], together with elemental mapping by electron probe microanalysis (EPMA) using a JEOL JXA-ISP100 equipped with a wavelength-dispersive spectrometer (WDS XM-3610XCE) to enhance the accuracy of micro-scale chemical composition analysis.

Phase identification and crystal structure analysis were conducted using X-ray diffraction (XRD) with a D8 ADVANCE (Bruker) instrument and a Cr-Kα radiation source in phase identification mode. The analyses were performed on specimens in the as-received condition, after solution nitriding, and after nitrocarburizing. In addition, the nitrocarburized specimens were further analyzed in thin film mode to investigate phase changes as a function of depth from the surface. This was done by sequential surface removal to depths of approximately 5 µm, 10 µm, 50 µm, and 100 µm, with measurements conducted at an incident angle of 5°.

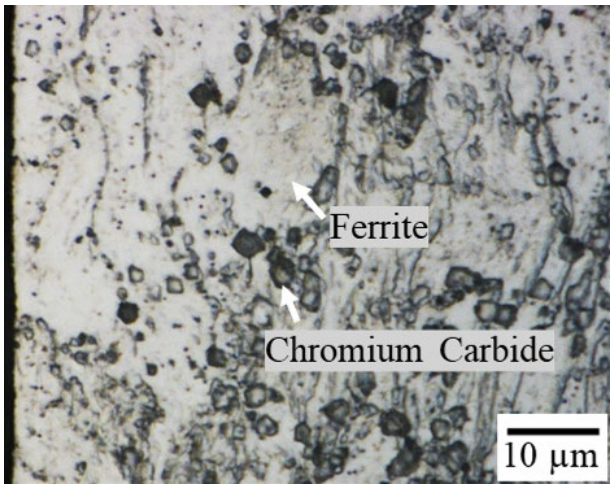


Figure 1. Microstructure of the as-received material (JIS SUS430).

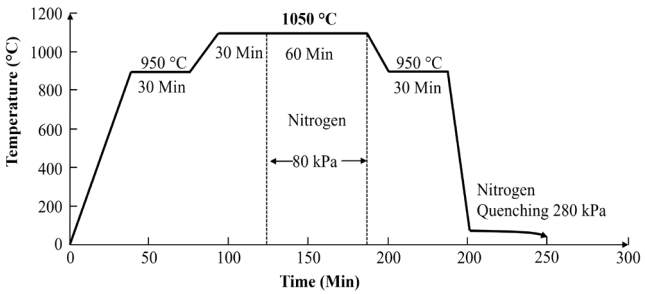


Figure 2. Solution Nitriding heat treatment conditions.

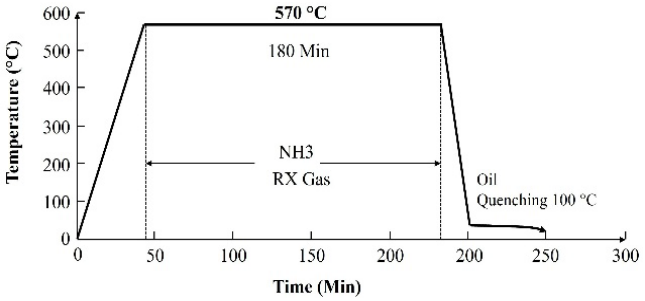


Figure 3. Nitrocarburizing heat treatment conditions.

Table 1. Chemical composition of SUS430 stainless steel.

SUS430	Chemical composition [wt%]							
	C	Si	Mn	P	S	Cr	Ni	Fe
JIS G 4305	≤0.12	≤0.75	≤1.00	≤0.040	≤0.030	16.00 to 18.00	-	Bal
Test specimen	0.09	0.28	0.82	0.030	0.004	16.44	0.38	Bal

Hardness testing was carried out using a Vickers micro-hardness tester (Future-Tech FM-800). A load of 0.30 kgf was applied for specimens after solution nitriding, while a lower load of 0.10 kgf [23] was used for measuring surface hardness and hardness profiles along the depth of specimens after nitrocarburizing to evaluate the thickness and characteristics of the diffusion layer [14]. Furthermore, the nitrocarburized specimens were additionally tested using a dynamic ultra micro hardness tester (DUH-211S) under a load of 50 mN [24] to assess the mechanical properties of the compound layer near the surface in greater detail.

Wear resistance was evaluated using a ball-on-disc tribometer (Bruker UMT TriboLab) under dry sliding conditions. The wear tests were performed on the as-received, solution-nitrided (SN), and solution-nitrided followed by gas nitrocarburizing (SN+NC) specimens using a ceramic ball as the counter body. A normal load of 5 N and a total sliding distance of 500 m were applied to all specimens. The wear behavior of each specimen was evaluated by comparing the wear tracks after testing. The wear test was conducted to investigate the influence of the combined thermochemical treatment on the tribological performance of SUS430 stainless steel and to correlate the wear behavior with the microstructure, phase evolution, and hardness of the treated surface.

3. Results and discussion

3.1 Microstructure

Microstructural images obtained from optical microscopy (OM) and scanning electron microscopy (SEM) revealed significant structural evolution after solution nitriding and nitrocarburizing treatments.

After solution nitriding, the surface region up to a depth of approximately 100 μm predominantly consisted of martensite, as shown in Figure 4 (a–b). Similar behavior has been reported previously [8,9], where nitrogen diffusion into the matrix promoted phase transformation during heat treatment. At greater depths, a mixed martensite-ferrite structure was observed continuously toward the core region, as shown in Figure 4 (c–d). This indicates the formation of a graded structure resulting from variations in nitrogen concentration and phase transformation behavior along the depth.

Following nitrocarburizing, the surface microstructure changed significantly, with the formation of a compound layer and an underlying diffusion layer, as shown in Figure 5(a), which is characteristic of thermochemical treatments involving simultaneous nitrogen and carbon diffusion [6,25]. The core region shown in Figure 5(b) retained the martensite–ferrite structure generated during the solution nitriding process, indicating that nitrocarburizing mainly modified the near-surface region without significantly affecting the substrate interior. During gas nitrocarburizing, nitrogen and carbon atoms diffuse into the pre-treated surface and interact with the iron- and chromium-containing matrix. The high defect density and lattice distortion associated with the martensitic region may enhance the accommodation of these interstitial atoms, contributing to the development of the compound and diffusion layers.

Higher-magnification SEM observations in Figure 5(c) revealed a compound layer thickness of approximately 5 μm, likely formed by the interaction of nitrogen and carbon with iron and chromium. Beneath this layer, a continuous diffusion layer extended to approximately 60 μm, consistent with previous reports [26]. This duplex-layer structure contributes to enhanced surface hardness and wear resistance through the combined effects of a hard compound layer and a supporting diffusion zone. The formation of the compound layer can be attributed primarily to the accumulation and reaction of nitrogen and carbon near the surface, whereas the underlying diffusion layer results from their penetration into the substrate. Thus, the multilayered structure reflects the concentration gradient and diffusion behavior of nitrogen and carbon during nitrocarburizing.

Overall, the results confirm the formation of a multilayered structure consisting of a compound layer, diffusion layer, and core microstructure. This graded structure plays an important role in improving the surface properties and mechanical performance of SUS430 stainless steel.

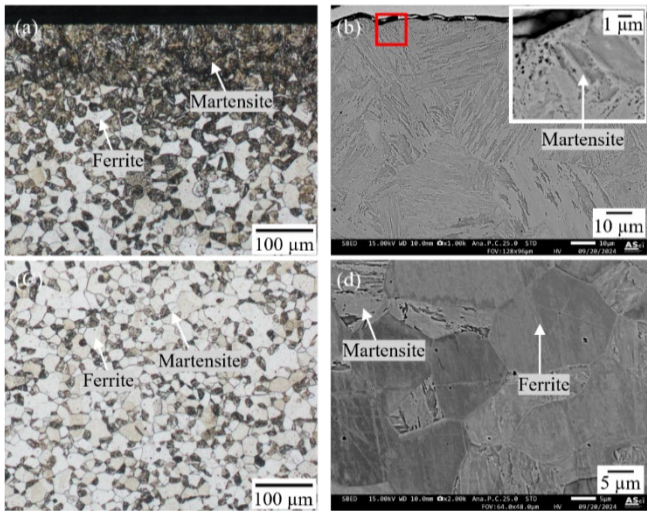


Figure 4. Microstructures at the surface and core of the specimen after solution nitriding: (a) Optical microstructure at the surface, (b) Scanning electron microscopy (SEM) at the surface, (c) Optical microstructure at the core, and (d) Scanning electron microscopy (SEM) at the core.

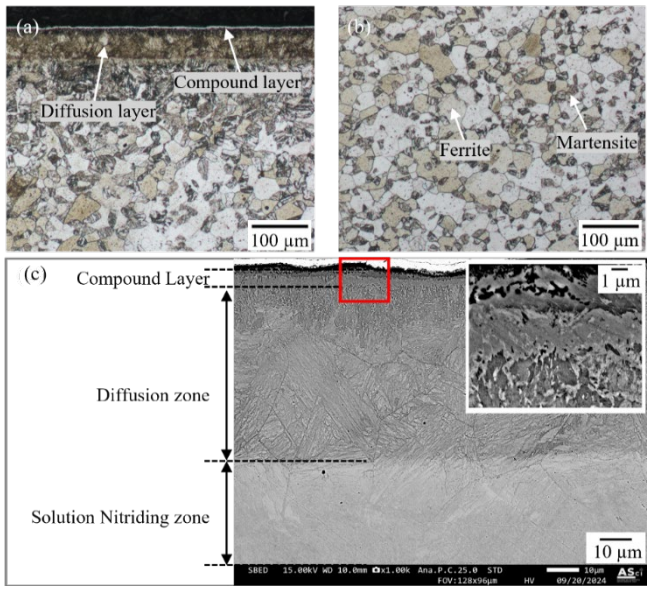


Figure 5. Microstructures at the surface and core of the specimen after nitrocarburizing: (a) Optical microstructure at the surface, (b) Optical microstructure at the core, and (c) Scanning electron microscopy (SEM) at the surface.

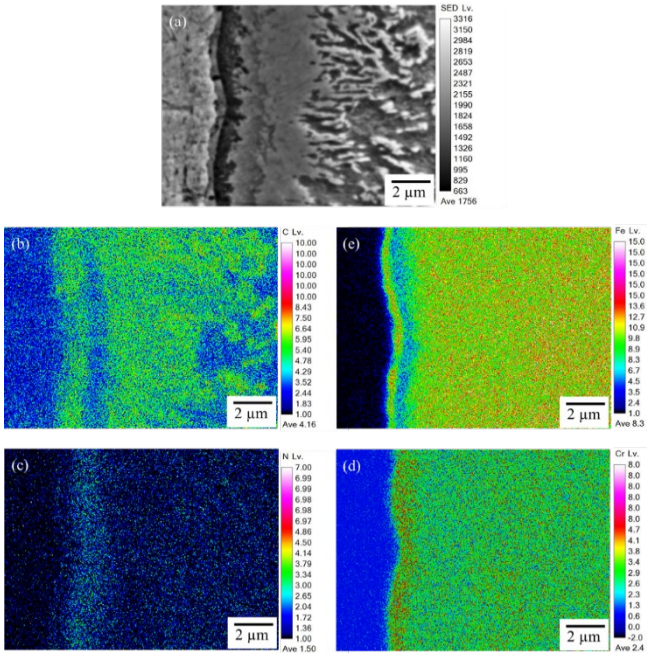


Figure 6. Microstructure of the nitrocarburized specimen and EPMA elemental mapping: (a) SEM image, (b) Elemental mapping of carbon, (c) Elemental mapping of nitrogen, (d) Elemental mapping of chromium, and (e) Elemental mapping of iron.

3.2 Compositional analysis

The chemical composition of the nitrocarburized specimens was analyzed using electron probe microanalysis (EPMA) combined with elemental mapping using a wavelength-dispersive spectrometer (WDS) under scanning electron microscopy (SEM) observation. The corresponding results are presented in Figure 6, focusing on the compound layer formed at the material surface.

The elemental mapping results reveal a clear compositional gradient from the surface toward the substrate. High concentrations of nitrogen and carbon were observed near the outermost surface together with chromium enrichment, indicating interactions between diffusing interstitial elements and alloying constituents, particularly iron and chromium. This behavior is consistent with previous studies on nitrocarburized stainless steels, which reported that the simultaneous diffusion of nitrogen and carbon promotes localized compositional modification and the development of surface layers during thermo-chemical treatment [26]. As the depth increases, the nitrogen concentration gradually decreases due to the reduction in diffusion driving force, whereas carbon remains distributed within the subsurface region and contributes to stabilizing the nitride and carbonitride phases formed. The observed nitrogen and carbon gradients also support the diffusion of these interstitial elements from the surface into the substrate during gas nitrocarburizing. The presence of chromium enrichment near the surface suggests that chromium may interact with the diffusing nitrogen and carbon, although the elemental mapping alone cannot identify the specific compounds formed.

Based on the observed elemental distribution, the formation of iron nitride phases such as ε- $Fe_{2-3}N$ and γ′-Fe_4N within the compound layer is considered possible, which is consistent with previous reports on nitrocarburized layers [27,28]. These phases are widely recognized for their contribution to high surface hardness and improved wear resistance [26]. In addition, chromium enrichment near the surface may promote the formation of chromium nitrides or carbonitrides, which can further improve thermal stability and strengthen the surface layer through precipitation strengthening mechanisms, as reported in previous studies [28]. However, it should be noted that EPMA elemental mapping cannot distinguish metallic Cr from Cr-containing compounds such as CrN. Therefore, the possible formation of CrN in this study is interpreted based on the combined evidence from XRD phase analysis [5,26], the co-distribution of Cr and N observed by EPMA, and previously reported results for nitrocarburized stainless steels, rather than from EPMA alone.

The possible formation of chromium nitrides may also contribute to surface hardening through precipitation strengthening and may influence the corrosion behavior by reducing the availability of chromium for the formation of a protective chromium-rich oxide film. However, because corrosion testing was not conducted in this study, the effect of chromium nitride formation on corrosion resistance cannot be directly confirmed and is discussed only based on phase analysis and previous literature.

Overall, the compositional variation with depth reflects the combined effects of nitrogen and carbon diffusion together with phase equilibrium established during heat treatment. The resulting graded compositional structure plays an important role in the development of a multilayered surface architecture and is closely associated with the enhancement of surface hardness discussed in the following section. These results support the proposed formation mechanism in which nitrogen and carbon diffuse into the modified surface region and react with the Fe- and Cr-containing matrix, contributing to the formation of the compound and diffusion layers.

3.3 Phase analysis

The X-ray diffraction (XRD) patterns of the specimen surfaces under different treatment conditions are presented in Figure 7, showing significant phase evolution after thermochemical treatments, consistent with previous studies [26,29]. The untreated SUS430 stainless steel exhibited predominantly ferrite peaks, corresponding to the base ferritic structure of the material.

After solution nitriding, the intensity of the ferrite peaks decreased significantly, accompanied by the appearance of nitrogen-expanded austenite peaks. Similar behavior has been reported in previous studies [29], where nitrogen diffusion into interstitial sites causes lattice distortion and alters phase stability, leading to phase transformation near the surface region

Following nitrocarburizing, the crystal structure became more complex, with the formation of iron nitrides together with chromium nitrides and indications of iron carbide phases. This behavior is attributed to the simultaneous diffusion of nitrogen and carbon. Previous studies have reported that hard phases such as ε- $Fe_{2-3}N$ and γ′-Fe4N play an important role in improving the surface hardness and wear resistance of nitrocarburized layers [26,28]. The formation of these hard nitride phases within the compound layer can contribute to surface hardening through phase strengthening, while carbon-containing phases may additionally contribute to the strengthening of the near-surface region. The combined presence of the compound

layer and underlying diffusion region therefore provides a metallurgical basis for the high surface hardness observed after nitrocarburizing.

Regarding the chromium-containing phases, the XRD results suggest the possible presence of chromium nitride phases in the nitrocarburized surface region. However, this identification should be interpreted with caution because the available EPMA elemental mapping provides information on the spatial distributions of Cr and N but cannot directly distinguish metallic chromium from CrN. Therefore, the possible formation of CrN is considered based on the combined interpretation of the XRD results, the co-distribution of Cr and N observed by EPMA, and previously reported phase formation in nitrocarburized stainless steels [28], rather than on EPMA evidence alone.

The phase evolution with depth from the surface is shown in Figure 8. The outermost surface region mainly consisted of iron nitride phases, while iron carbide phases began to appear at depths of approximately 5 μm to 10 μm, reflecting the influence of carbon within the diffusion layer. At greater depths of approximately 50 μm and 100 μm, the intensities of nitride and carbide phases gradually decreased, whereas ferrite peaks became more dominant, indicating a transition toward the original substrate structure. This depth-dependent phase distribution is consistent with the concentration gradients of nitrogen and carbon observed by EPMA, indicating that the formation of the surface phases is closely related to the diffusion and decreasing concentrations of these interstitial elements with increasing depth.

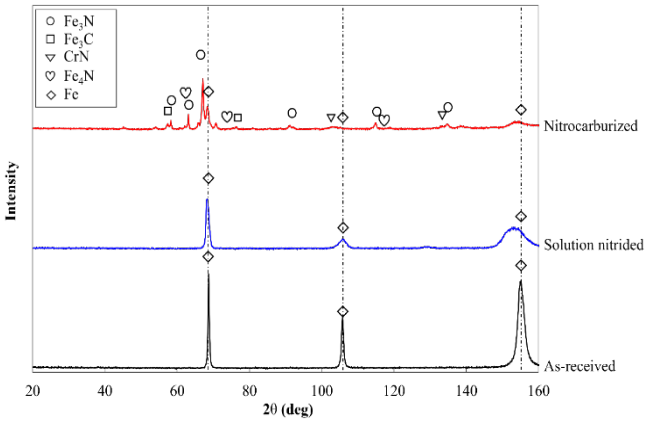


Figure 7. XRD patterns of SUS430 under different heat-treatment conditions.

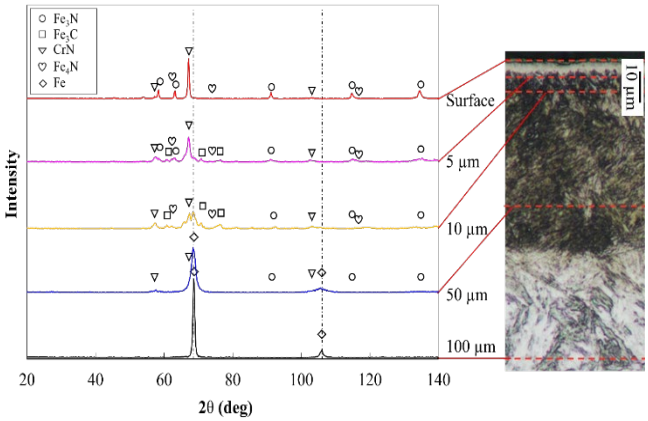


Figure 8. Depth-dependent XRD diffractograms of SUS430 samples after nitrocarburizing.

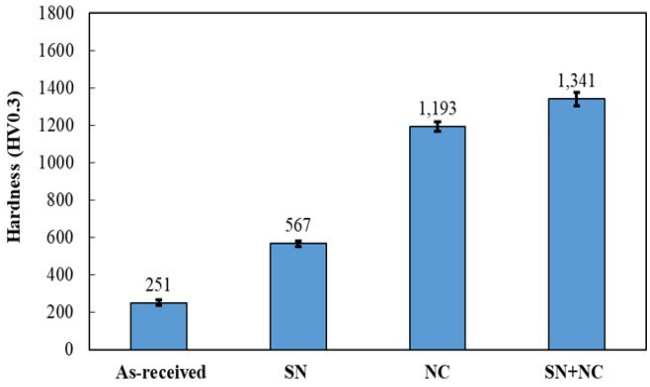


Figure 9. Surface hardness of specimens under different heat-treatment conditions.

Overall, the observed phase evolution reflects the combined effects of nitrogen and carbon diffusion together with phase equilibrium during heat treatment, resulting in a graded multilayer structure that plays an important role in enhancing the mechanical properties of the surface layer. The formation of iron nitrides and the possible formation of chromium nitrides provide additional strengthening mechanisms, including phase strengthening and possible precipitation strengthening. However, the contribution of chromium nitrides to corrosion behavior cannot be directly established from the present results because no electrochemical corrosion measurements were performed in this study.

3.4 Hardness

The surface hardness after heat treatment is shown in Figure 9. The results indicate a significant increase in hardness following each surface modification process. After solution nitriding (SN), the surface hardness increased to 567 HV, or approximately 2.25 times higher than that of the untreated specimen. This improvement is attributed to the interstitial diffusion of nitrogen, which distorts the crystal lattice and increases resistance to dislocation movement, resulting in hardness comparable to that of martensite. For comparison, the specimen treated by gas nitrocarburizing alone (NC) exhibited a surface hardness of 1193 HV, whereas the specimen subjected to the combined solution nitriding and gas nitrocarburizing treatment (SN+NC) exhibited a higher surface hardness of 1341 HV. The higher hardness obtained after SN+NC indicates that solution nitriding provides an additional surface-hardening benefit compared with gas nitrocarburizing alone.

After nitrocarburizing, the surface hardness further increased to 1341 HV, which is about 2.36 times higher than that after solution nitriding and approximately 5.33 times higher than that of the untreated specimen. This substantial increase is due to the formation of a compound layer consisting of iron nitrides and carbides, along with precipitation and compressive residual stresses near the surface. The increase in hardness should not be attributed to the compound layer alone. The high hardness after SN+NC is considered to result from the combined effects of the pre-existing martensite structure [9,17], lattice distortion caused by interstitial nitrogen and carbon, strengthening associated with iron nitride formation, the possible formation of chromium nitrides, and compressive residual stresses generated during thermochemical treatment. The martensite layer formed during solution nitriding provides a harder supporting microstructure, while the

subsequent incorporation of nitrogen and carbon and formation of hard nitride phases further strengthen the near-surface region [26].

Among these mechanisms, the contribution of the compound layer is expected to be particularly important for the very high surface hardness, while the underlying diffusion layer and martensitic substrate provide mechanical support and contribute to load bearing. However, the individual contribution of each strengthening mechanism can not be quantitatively separated using the present experimental data.

The increasing hardness trend is consistent with the development of a multilayered surface structure, driven by diffusion mechanisms and the formation of nitride and carbide phases. These factors play a key role in controlling the mechanical properties of the material. The higher hardness of SN+NC compared with NC alone suggests that the microstructural modification produced by solution nitriding may provide favorable conditions for subsequent nitrogen and carbon incorporation during gas nitrocarburizing. Thus, the results demonstrate the additional benefit of using solution nitriding as a pre-treatment before gas nitrocarburizing.

Figure 10 shows the relationship between hardness and the distance from the specimen surface. The untreated material exhibited relatively constant hardness throughout the cross-section, reflecting a homogeneous microstructure. In contrast, the heat-treated specimens showed the highest hardness at the surface, which gradually decreased with increasing depth. This behavior is consistent with the diffusion mechanism of interstitial elements and the microstructural changes occurring during thermochemical treatment [6,26].

The total case depth after solution nitriding was approximately 140 µm, whereas that after nitrocarburizing was about 70 µm. It should be noted that these two case-depth values represent different metallurgical characteristics and therefore should not be directly compared as equivalent measures of diffusion depth. The approximately 140 µm depth after solution nitriding corresponds to the region in which the original ferritic structure was transformed into a martensitic structure during the high-temperature solution nitriding process. In contrast, the approximately 70 µm depth after nitrocarburizing represents the hardened region determined from the hardness profile, which is associated mainly with the compound layer and underlying diffusion layer formed during nitrocarburizing. Therefore, the smaller hardened depth after nitrocarburizing does not indicate a reduction or loss of the martensitic region previously formed by solution nitriding.

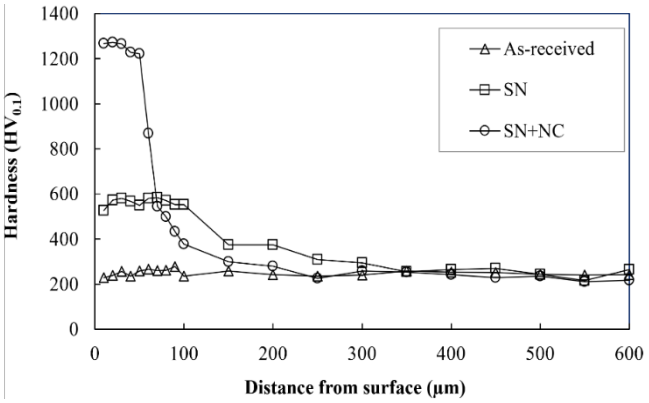


Figure 10. Distributions of the hardness values under different heat-treatment conditions.

The increase in surface hardness is associated with the formation of a compound layer and a diffusion layer, as illustrated in Figure 11. The compound layer, consisting of hard nitride and carbonitride phases, contributes to improved surface hardness and wear resistance, while the diffusion layer enhances load-bearing capability and provides a gradual transition in mechanical properties [6,27]. In the SN+NC condition, the pre-existing martensitic region formed during solution nitriding remains beneath the nitrocarburized surface layers and provides additional mechanical support. Thus, the final hardened structure consists of a hard near-surface compound layer, an underlying diffusion layer, and the pre-existing martensitic/ferritic substrate [26].

The gradual decrease in hardness with depth is also consistent with the EPMA and XRD results, which revealed a reduction in nitrogen and carbon concentrations together with phase changes from the surface toward the substrate. This depth-dependent hardness profile reflects the decreasing concentration of diffused interstitial elements and the corresponding reduction in the amount of hardened phases with increasing distance from the surface.

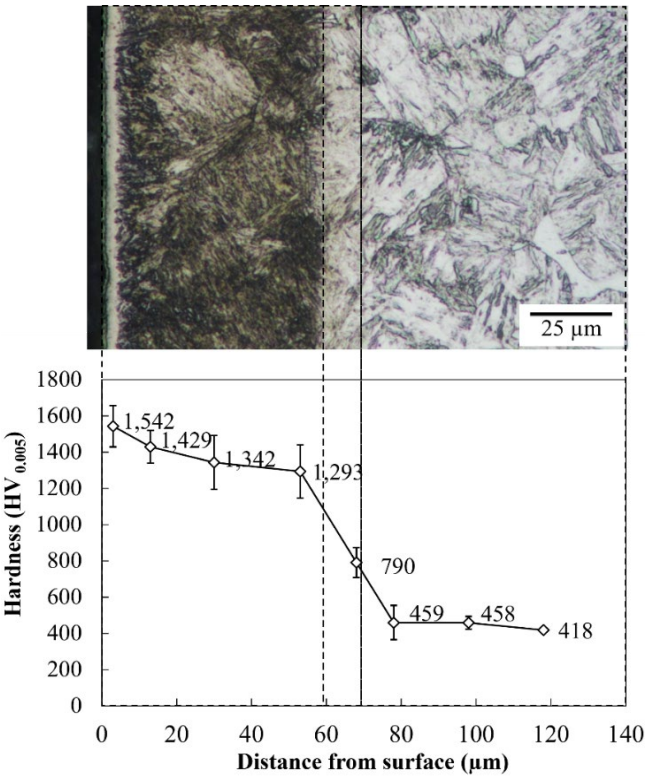


Figure 11. Distributions of the hardness values in depth after nitrocarburizing.

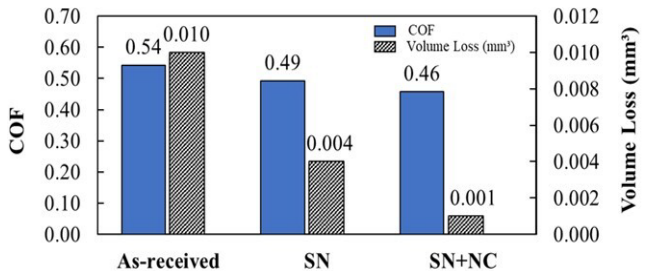


Figure 12. Wear volume and coefficient of friction (COF) of specimens under different heat-treatment conditions.

Overall, the results indicate that solution nitriding plays an important role in modifying the initial microstructure and controlling diffusion behavior during the subsequent nitrocarburizing process, leading to the development of a multilayered surface structure that effectively enhances the mechanical properties of the material surface. The comparison of the two case-depth values should therefore be interpreted in terms of their respective metallurgical definitions rather than as a direct comparison of the diffusion capability of solution nitriding and nitrocarburizing.

3.5 Wear behavior

Figure 12 shows the wear volume and coefficient of friction (COF) of the as-received, solution-nitrided (SN), and solution-nitrided followed by gas nitrocarburizing (SN+NC) specimens. The wear volume decreased from the as-received condition after solution nitriding and decreased further after the combined SN+NC treatment. The SN+NC specimen showed the lowest wear volume, indicating the highest wear resistance among the tested specimens. Similarly, the COF decreased from 0.54 for the as-received specimen to 0.49 after solution nitriding and further to 0.46 after the SN+NC treatment, indicating improved tribological performance.

The improvement in wear resistance is consistent with the hardness results presented in Figure 9. Although solution nitriding increased the surface hardness through martensitic transformation, the subsequent gas nitrocarburizing treatment further improved the wear resistance through the formation of a compound layer and diffusion layer. These surface layers contributed to reducing material loss during sliding and lowering the coefficient of friction.

The improved wear resistance is also consistent with the XRD and EPMA results, which showed iron nitride phases and the possible formation of chromium-containing nitrides, together with a graded distribution of nitrogen and carbon beneath the surface. These changes in microstructure and phase composition may increase the resistance of the surface to deformation during sliding, resulting in lower wear volume and coefficient of friction.

The improved wear performance of the SN+NC specimen is therefore attributed to the contribution of the martensitic layer formed during solution nitriding together with the compound and diffusion layers formed during gas nitrocarburizing. Compared with the as-received specimen, the combined treatment resulted in lower wear volume and coefficient of friction, indicating improved tribological performance. These results demonstrate that the combined treatment improves the tribological performance of SUS430 stainless steel under the present test conditions.

4. Conclusions

This study investigated the development of microstructure and mechanical properties of SUS430 stainless steel after solution nitriding and nitrocarburizing. The analyses included microstructure, chemical composition, crystal structure, and hardness. The conclusions are summarized as follows.

(1) Microstructure Solution nitriding resulted in the formation of a martensitic structure near the surface to a depth of approximately 100 μm, gradually transitioning to a mixed martensite–ferrite structure toward the core, forming a graded structure along the depth. After nitrocarburizing, a multilayered structure was formed, consisting of a compound layer with a thickness of about 5 μm and a diffusion layer extending to approximately 60 μm. The core retained its original structure, indicating that this process improves surface properties without significantly affecting the internal structure. The martensite layer formed during solution nitriding exhibits a modified microstructure with lattice distortion and a high density of defects, which may provide favorable conditions for the subsequent incorporation and diffusion of nitrogen and carbon during gas nitrocarburizing.

(2) Chemical composition EPMA/WDS analysis showed a gradient distribution of nitrogen and carbon from the surface into the interior. The compound layer exhibited a high concentration of N and C together with Fe and Cr, indicating the formation of hard nitride phases such as ε-$Fe_{2-3}N$ and γ′-Fe_4N, as well as the possible formation of chromium nitrides. However, EPMA/WDS elemental mapping cannot directly distinguish metallic Cr from CrN. Therefore, the possible formation of chromium nitrides is interpreted from the combined evidence of XRD phase analysis, the co-distribution of Cr and N observed by EPMA, and previously reported results, rather than from EPMA alone. These phases contribute to improved stability and wear resistance of the surface layer.

(3) Crystal structure XRD results revealed a sequential phase transformation from ferrite in the base material to nitrogen-expanded austenite after solution nitriding, and further to a multiphase structure consisting of iron nitrides, iron carbides, and chromium nitrides after nitrocarburizing. Depth profile analysis confirmed that the fraction of nitride and carbide phases decreases with increasing depth from the surface, consistent with the diffusion behavior of nitrogen and carbon and the formation of a graded multilayer structure. The formation of hard nitride and carbide phases provides an important contribution to surface strengthening and is consistent with the high surface hardness obtained after the combined treatment.

(4) Mechanical properties Surface hardness increased significantly following each treatment step. After solution nitriding, the hardness reached 567 HV (approximately 2.25 times that of the base material), and further increased to 1341 HV after nitrocarburizing (approximately 5.33 times that of the base material). For comparison, gas nitrocarburizing alone resulted in a surface hardness of 1193 HV, whereas the combined SN+NC treatment achieved 1341 HV, demonstrating the additional benefit of solution nitriding as a pre-treatment. The maximum hardness was observed at the surface and decreased with depth, consistent with the total case depth of approximately 140 μm for solution nitriding and 70 μm for nitrocarburizing. These two case-depth values represent different metallurgical characteristics: the approximately 140 μm depth after solution nitriding corresponds to the martensitic transformation region, whereas the approximately 70 μm depth after nitrocarburizing represents the hardened region determined from the hardness profile. Therefore, these values should not be directly compared as equivalent measures of diffusion depth.

The increase in hardness is not attributed to the compound layer alone but is considered to result from the combined effects of the pre-existing martensitic structure, lattice distortion caused by interstitial nitrogen and carbon, strengthening associated with nitride and carbide phases, the possible formation of chromium nitrides, and compressive residual stresses. The compound layer provides high surface hardness,

while the underlying diffusion layer and martensitic region provide mechanical support and load-bearing capability. However, the individual contribution of each strengthening mechanism cannot be quantitatively separated based on the present experimental data.

In summary, the solution nitriding process serves as an important pre-treatment step for preparing the microstructure prior to nitrocarburizing. It promotes the formation of a multilayered microstructure, including both a compound layer and various phases. No porosity was observed in the compound layer, which differs from the typical white layer formed in conventional nitrocarburizing processes that often contains some porosity. This structure works effectively to enhance surface hardness and potentially wear resistance, reflecting the mechanistic relationship between the base material, element diffusion, and systematic control of surface mechanical properties. The direct wear test further demonstrated that the SN+NC specimen exhibited the lowest wear volume and coefficient of friction (COF), supporting the improvement in tribological performance obtained by the combined treatment. These results demonstrate the additional engineering benefit of using solution nitriding as a pre-treatment prior to gas nitrocarburizing compared with gas nitrocarburizing alone.

Regarding corrosion resistance, this study did not include direct electrochemical measurements. Therefore, no definitive conclusion regarding an increase or decrease in corrosion resistance can be drawn from the present experimental results. Any possible change in corrosion behavior is discussed only based on the observed phase evolution, EPMA results, and previously reported effects of chromium nitride formation on corrosion behavior. Further investigation using electrochemical techniques, such as potentiodynamic polarization and electrochemical impedance spectroscopy (EIS), is recommended to quantitatively evaluate the corrosion performance of the treated SUS430 stainless steel.

Acknowledgements

The authors would like to express their sincere gratitude to Thai Tohken Thermo Co., Ltd. for their support in providing materials, equipment, and facilities, as well as their technical assistance in experimental data collection and analysis. The authors also sincerely thank Dr. Sankum Nusen and Dr. John T.H. Pearce of Chiang Mai University, Thailand, for their valuable and insightful discussions.

References

[1] M. K.-A. Hassan Nasri Nasrabadi, and K. Amini, "Investigation of dissimilar joining ferritic stainless steel 430 to austenitic stainless steel 304 by transient liquid phase bonding process," *Journal of Metals, Materials and Minerals,* vol. 29, pp. 8–15, 2019.

[2] J. Alphonsa, S. Mukherjee, and V. S. Raja, "Study of plasma nitriding and nitrocarburising of AISI 430F stainless steel for high hardness and corrosion resistance," *Corrosion Engineering, Science and Technology,* vol. 53, no. sup1, pp. 51–58, 2018.

[3] T. Thublaor, P. Srihathai, P. Wiman, A. Muengjai, and S. Chandra-Ambhorn, "Oxidation behaviour of Mn-Co spinel coating on AISI 430 ferritic stainless steel with and without Cu in Ar-CO_2-H_2O atmosphere," *Journal of Metals, Materials and Minerals,* vol. 33, no. 2, pp. 29–37, 2023.

[4] P. Ngamsri, S. Pokwitidkul, P. Treewiriyakitja, P. Thongyoug, R. Nilprapa, and J. Tungtrongpairoj, "The high temperature degradation of ferritic stainless steel in solid carbon atmospheres," *Journal of Metals, Materials and Minerals,* vol. 33, no. 1, pp. 8–13, 2023.

[5] Y. Wang, M. Li. D. Zhang, and M. Xia "Study on surface nitriding treatment of the sinter," *Journal of Physics: Conference Series,* vol. 2553, p. 012034, 2023.

[6] H. Aydin, A. Bayram, and Ş. TopÇU, "Friction characteristics of nitrided layers on AISI 430 ferritic stainless steel obtained by various nitriding processes," *Materials Science,* vol. 19, no. 1, 2013.

[7] F. Eskandari, M. Atapour, M. A. Golozar, B. Sadeghi, and P. Cavaliere, "The microstructure and wear behaviour of friction stir processed AISI 430 ferritic stainless steel," *Tribology - Materials, Surfaces & Interfaces,* vol. 13, no. 3, pp. 172–181, 2019.

[8] H. Berns, J. W. Bouwman, U. Eul, J. Izagirre, R. L. Juse, H. J. Niederau, G. Tavernier, and R. Zieschang, "Solution nitriding of stainless steels for process engineering," *Materialwissenschaft und Werkstofftechnik,* vol. 31, no. 2, pp. 152–161, 2000.

[9] J.-M. K. Sang-Jun Park, H.-J. Kang, C.-Y. Kang, Y.-H. Kim, and J.-H. Sung, "Isothermal heat treatment of AISI 430 ferritic stainless steel after high temperature gas nitriding" *Journal of the Korean Society for Heat Treatment,* vol. 25, no. 3, pp. 115–120, 2012.

[10] C. X. Li, and T. Bell, "A comparative study of low temperature plasma nitriding, carburising and nitrocarburising of AISI 410 martensitic stainless steel," *Materials Science and Technology,* vol. 23, no. 3, pp. 355–361, 2007.

[11] H. Du, M. A. J. Somers, and J. Agren, "Microstructural and compositional evolution of compound layers during gaseous nitrocarburizing," *Metallurgical and Materials Transactions A,* vol. 31, no. 1, pp. 195–211, 2000.

[12] H. Du, and M. A. J. Somes, and J. Ågren, "Theoretical treatment of nitriding and nitrocarburizing of iron," *Metallurgical and Materials Transactions,* vol. 27, pp. 1073–1080, 1996.

[13] J. Ratajski, J. Tacikowski, and M. A. J. Somers, "Development of compound layer of iron (carbo)nitrides during nitriding of steel," *Surface Engineering,* vol. 19, no. 4, pp. 285–291, 2003.

[14] A. Holst, S. Kante, A. Leineweber, and A. Buchwalder, "Mechanism of layer formation during gas nitriding of remelted ledeburitic surface layers on unalloyed cast irons," *Metals,* vol. 13, no. 1, p. 156, 2023.

[15] E. Ghelloudj, "Investigation of the effect of nitrocarburizing treatment on tribological properties of Aisi 1045 medium carbon steel," *Acta Metallurgica Slovaca,* vol. 28, no. 1, pp. 5–9, 2022.

[16] W. Tuckart, M. Gregorio, and L. Iurman, "Sliding wear of plasma nitrided AISI 405 ferritic stainless steel," *Surface Engineering,* vol. 26, no. 3, pp. 185–190, 2010.

[17] T. L. Christiansen, M. Villa, C. Tibollo, K. V. Dahl, and M. A. J. Somers, "High temperature solution nitriding of stainless steels; Current status and future trends," *HTM Journal of Heat Treatment and Materials,* vol. 75, no. 2, pp. 69–82, 2020.

[18] N. Nakamura, and S. Takaki "Structural control of stainless steel by nitrogen absorption in solid state," *ISIJ International,* vol. 36, no. 7, pp. 922–926, 1996.

[19] B. Valmik, K. Prakash, S. Jagdish, S. Digvijay, and R. K. P. Singh, "Influence of medium used during ferritic nitro-carburizing of AISI H-13 hot work tool steel," *Journal of Materials Science and Engineering A,* vol. 8, no. 1, 2018.

[20] P. C. King, R. W. Reynoldson, A. Brownrigg, and J. M. Long, "Ferritic nitrocarburising of tool steels," *Surface Engineering,* vol. 21, no. 2, pp. 86–98, 2005.

[21] N. Thammachot, N. Taweejun, T. Praditja, and W. Homjabok, "Effects of nitrocarburization on the surface morphology and tribology of SKH51 high-speed tool steel," *Journal of Materials Engineering and Performance,* vol. 33, no. 19, pp. 10415–10425, 2023.

[22] D. Tang, C.Zhang, H. Zhan, W. Huang, Z. Ding, D. Chen, and G. Cui, "High-efficient gas nitridation of AISI 316L austenitic stainless steel by a novel critical temperature nitriding process," *Coatings,* vol. 13, no. 10, p. 1708, 2023.

[23] G. P. Singh, J. Alphonsa, P. K. Barhai, P. A. Rayjada, P. M. Raole, and S. Mukherjee, "Effect of surface roughness on the properties of the layer formed on AISI 304 stainless steel after plasma nitriding," *Surface and Coatings Technology,* vol. 200, no. 20-21, pp. 5807–5811, 2006.

[24] K. Köster, P. Kaestner, G. Bräuer, H. Hoche, T. Troßmann, and M. Oechsner, "Material condition tailored to plasma nitriding process for ensuring corrosion and wear resistance of austenitic stainless steel," *Surface and Coatings Technology,* vol. 228, pp. S615–S618, 2013.

[25] Z. Xi, Q. Jing, Y. Wang, X. Han, R. He, and H. Zhang, "Influence of nitriding treatment on the microstructure and mechanical properties of AISI 422 martensitic stainless steel," *Materials & Design,* vol. 257, Art. no. 114386, 2025.

[26] J. Zuo, W. Wang, and X. Zhang, "Study on vacuum gas nitriding process and surface properties of AISI 430 stainless steel," *Surface Science and Technology,* vol. 4, no. 1, Art. no. 10, 2026,

[27] M. A. Fontes, V. H. B. Scheid, D. d. S. Machado, L. C. Casteletti, and P. A. d. P. Nascente, "Morphology of the DIN 100Cr6 case hardened steel after plasma nitrocarburizing process," *Materials Research,* vol. 22, no. 3, 2019.

[28] R. L. O. Basso, R. J. Candal, C. A. Figueroa, D. Wisnivesky, and F. Alvarez, "Influence of microstructure on the corrosion behavior of nitrocarburized AISI H13 tool steel obtained by pulsed DC plasma," *Surface and Coatings Technology,* vol. 203, no. 10-11, pp. 1293–1297, 2009.

[29] B. Wang, T. L. Christiansen, and M. A. J. Somers, "Influence of ferrite-austenite distribution in 2205 duplex stainless steel on high-temperature solution nitriding behaviour," *Surface and Coatings Technology,* vol. 453, Art. no. 129134, 2023.